

# ECE 299 Holography and Coherent Imaging

Lecture 10. Swept Source and FD OCT

David J. Brady  
Duke University

# Outline

- Huang paper
- Tomography
- OCT and light-in-flight holography
- Mathematical model of OCT
- K-space analysis of OCT
- K-space analysis of 3D imaging
- Synthetic aperture OCT
- Diffraction tomography

# 2003 Paper

## **Sensitivity advantage of swept source and Fourier domain optical coherence tomography**

**Michael A. Choma, Marinko V. Sarunic, Changhuei Yang, Joseph A. Izatt**

*Department of Biomedical Engineering, Duke University, Durham, NC 27708*  
[jizatt@duke.edu](mailto:jizatt@duke.edu)

Michael Choma, Marinko Sarunic, Changhuei Yang, and Joseph Izatt, "Sensitivity advantage of swept source and Fourier domain optical coherence tomography," *Opt. Express* **11**, 2183-2189 (2003)

# SS-OCT system model

$$P_{D_i}(\vec{k}) = \langle |E_{D_i}(\vec{k})|^2 \rangle = S(\vec{k})R_R + S(\vec{k})R_S + 2S(\vec{k})\sqrt{R_R R_S} \cos(2k\Delta x + \varphi_i). \quad (1)$$

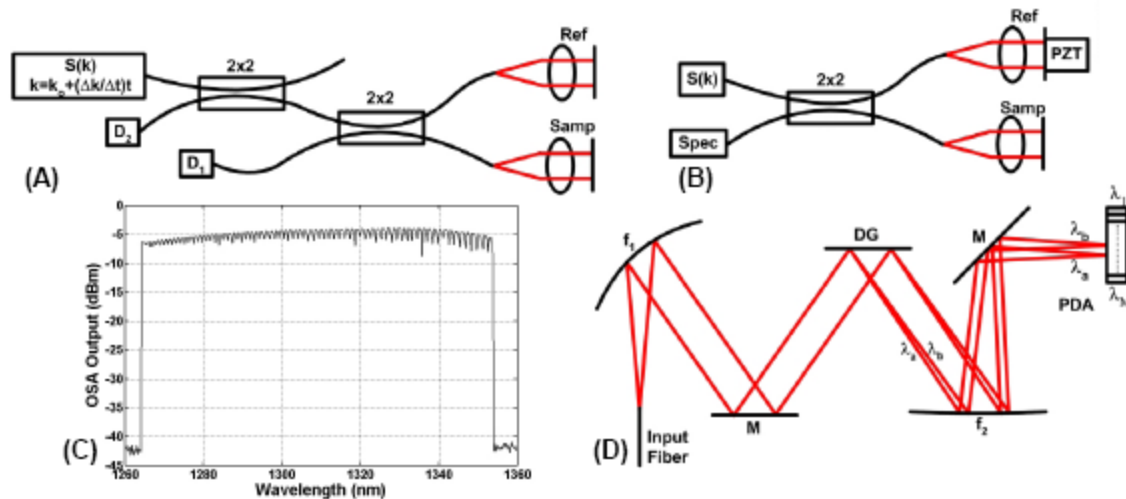
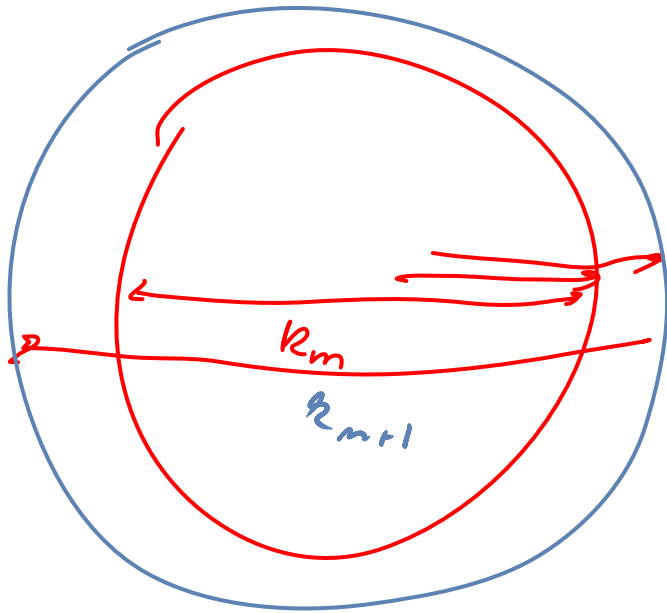


Fig. 1. A) Differential SS-OCT setup. The output of detectors 1 and 2 are differenced in software. B) Differential FD-OCT setup. Differential detection is accomplished by dithering the phase of the reference arm field by  $180^\circ$  with a piezo-mounted mirror on alternate scans. C) Swept source output measured with an optical spectrum analyzer (OSA). The apparent modulation appearing in the OSA plot is an artifact of spectral resolution and sweep time setting of the OSA. D) Czerny-Turner grating spectrometer (Spec) employed in FD-OCT system. D, detector; DG, diffraction grating;  $f$ , focal length of reflective optical element; M, mirror; PDA, photodiode array; PZT, piezoelectric actuator.

# SS-OCT acquisition model

$$k = k_0 + t(\Delta k / \Delta t),$$

$$D_i[k_m] = \frac{1}{2^i} \rho S[k_m] (R_R + R_S + 2\sqrt{R_R R_S} \cos(2k_m \Delta x + \varphi_i)).$$



The aim of SS-OCT is to obtain a depth-reflectivity profile  $D[x_n]$  of the sample arm. This can be obtained by discrete Fourier transforming any  $D_i[k_m]$  to obtain [2]

$$D[x_n] = \sum_{m=1}^M D_i[k_m] \text{Exp}[-j2k_mx_n]. \quad (3)$$

The factor of 2 in the kernel exponent ensures the recovery of single-sided distances, and  $n \in \{1, M\}$ . In the x-domain, the channel spacing is  $\delta x = \pi / \Delta k$  and the scan depth is  $\Delta x_{max} = \pi / \delta k$  [ $-\pi / (2\delta k)$  to  $+\pi / (2\delta k)$ ]. Because  $D[k_m]$  is real-valued, Eq. (3) yields an A-scan in which  $D[+x]$  and  $D[-x]$  are complex conjugate pairs. Thus, the effective scan depth is  $\Delta x_{max} = \pi / (2\delta k)$ . The design equation for the number of samples is  $M = 2\Delta x_{max} \Delta k / \pi$ , giving typical values of  $M \sim 10^2 - 10^3$ . The A-scan axial resolution is  $4 \ln 2 / \Delta k_{fwhm}$  using a Gaussian source with a full width-half maximum bandwidth  $\Delta k_{fwhm}$  [11], while the resolution is  $\pi / \Delta k$  using a rectangular source. Qualitatively, Eq. (3) has three peaks in the case of a single sample reflector. One peak represents the Fourier transform of  $S(k)$ , and is centered at  $x=0$ . The two other peaks sit at  $x_n = \pm \Delta x$ , and are due to the interferometric portion of Eq. (3).

# Quadrature detection

$$D[x_n] = \sum_{m=1}^M \left[ (D^0[k_m] - D^{\text{DC}}[k_m]) + j(D^{90}[k_m] - D^{\text{DC}}[k_m]) \right] \text{Exp}[-j2 k_m x_n].$$

# Noise

$$D(k_m) = |R + S|^2$$

$$\sigma[k_m] = (2e\dot{D}[k_m]B_{ssoct})^{1/2}$$

$$\sigma_x = \sqrt{\sum_{m=1}^M \sigma^2[k_m]} = \sqrt{e\rho R_R S_{ssoct} B_{ssoct}}$$

$$\text{SNR}_{ssoct} = \frac{\rho R_S S_{ssoct}}{4eB_{ssoct}} \approx M \frac{\rho R_S S_{idoct}}{4eB_{ssoct}}$$

$$D[x_n = \pm \Delta x] = \frac{1}{2} \rho \sqrt{R_R R_S} \sum_{m=1}^M S[k_m] = \frac{1}{2} \rho \sqrt{R_R R_S} S_{ssoct} \quad S_{ssoct} \approx M S_{idoct} \cdot 1$$



# Bandwidth

$$D[k_m] \propto \cos(2t \Delta x \Delta k / \Delta t),$$

$$B_{\text{SFOCT}} = \Delta k \Delta x_{\text{max}} / (\pi \Delta t).$$

$$\text{SNR}_{\text{SFOCT}} = \frac{\rho R_S S_{\text{SFOCT}}}{2 e B_{\text{SFOCT}}}.$$

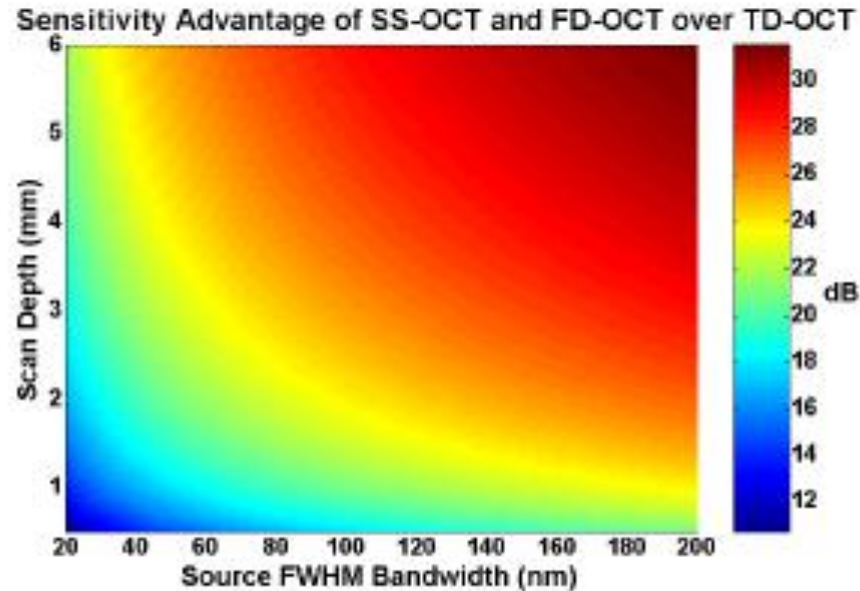


Fig. 2. Sensitivity advantage of SS-OCT and FD-OCT over conventional TD-OCT with a Gaussian source at 1300nm. Sensitivity advantage is defined as  $\text{SNR}_{\text{ss/oct}}/\text{SNR}_{\text{td/oct}}$  and expressed in dB.

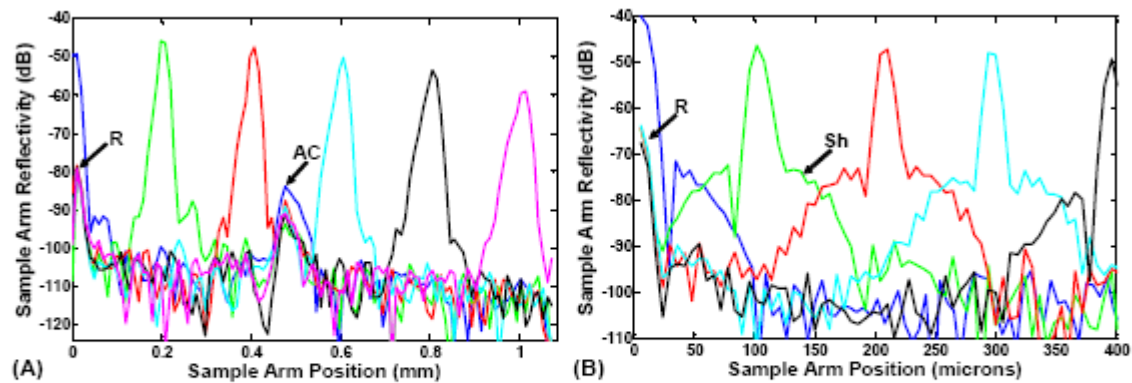
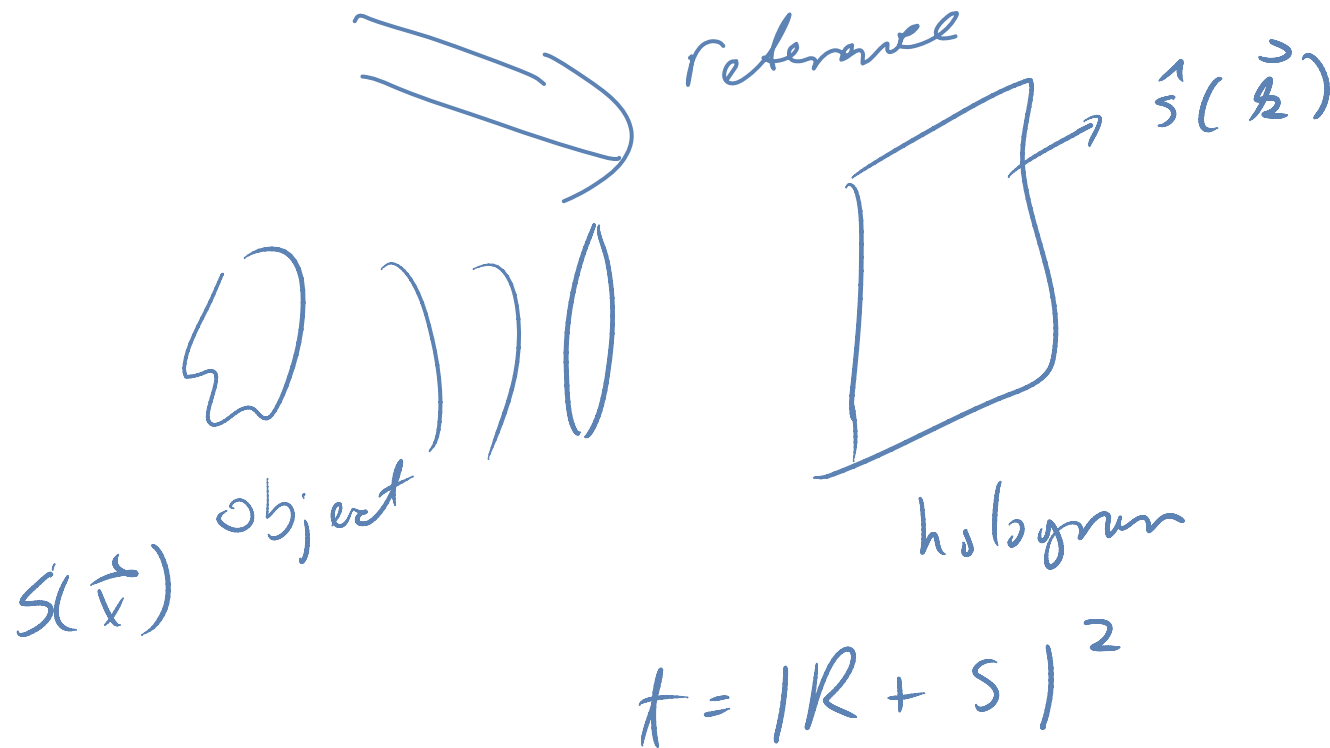


Fig. 3. A) SS-OCT peaks from a calibrated -47dB reflector at 200µm spacing increments. B) FD-OCT peaks from a calibrated -38dB reflector at 100µm increments. The shoulders (Sh) are artifacts of interpolation of the data from wavelength to wavenumber [16]. Imperfections in software differencing lead to residual DC (R) and autocorrelation (AC) peaks.

# What is the SNR for holographic sensing? How does holographic SNR compare to focal imaging?



# Are there coding alternatives for SS-OCT?